Micro CT measurements of defects in light-weighted mirrors for applications in space imaging

Peter A Cooper, Wenjuan Sun, Stephen B Brown

National Physical Laboratory

London, TW11 OLW, United Kingdom

02089 436525

peter.cooper@npl.co.uk

Carolyn Atkins

Science and Technology Facilities Council, United Kingdom

Abstract

An additively manufactured aluminium alloy light-weighted mirror sample was measured using micro X-ray computed tomography. The additive manufactured surface is polished or diamond turned to an optical surface quality, thus reducing surface defects is critical. The measurement was processed to investigate porosity in the sample which can become surface defects following the polishing or turning. The porosity was most prevalent in bands approximately 0.5 mm below the original surface and in areas away from the support columns. Porosity detection was found to be sensitive to threshold parameters showing the requirement for robust algorithms.

1 Introduction

With the demand to reduce weight in space based instrumentation, light-weighting of mirrors is an active area of research. Although conventional light weighting strategies such as contoured back, open back and sandwiching exist, manufacturing limitations mean these are not able to offer the full potential of optimized light-weighting. Additive manufacturing (AM), is the technique where layers of material, which can be metal or plastic, are built up using techniques such as electron beam manufacturing (EBM), or selective laser melting (SLM).The nature of AM means complex three dimensional (3D) support structures can be produced to give higher stiffness and strength to weight ratio[1]. Atkins *et al* have produced mirror structures and demonstrated the potential to achieve 3.6 nm average roughness (RMS) using a diamond turning process[2]. By optimizing the light weighting structure, a weight reduction of 18 % was achieved, using AM, while at the same time reducing form error in the surface.

While AM is a promising manufacturing technique it has associated challenges not present in conventional machining. These include defects such as porosity which can have multiple physical causes[3]. The strategy and parameters of the build process have a strong effect on the nature of these defects[4].

When the optical surface is produced during a finishing process the quality of the final surface will be highly dependent on the density and homogeneity of the material. This is because any pores or inclusions will be transformed to surface defects once the surface is polished or diamond turned. Quantifying the volume defects of the AM build before surface processing saves time and allows optimisation of the build. Once an acceptable build is made the defect information can be used to select the optimum depth of material to be removed during processing to minimise the interaction defects have with the surface. One of the few techniques with the potential to image internal defects is micro X-ray computed tomography scanning (µCT)[5].

µCT uses X-ray imaging from multiple angles to build a 3D structure of the density of the component. This can be used to check the integrity of the support structure build as well as examine any porosity or material defects. µCT has previously been reported for analysing porosity in titanium alloys produced using SLM[6]. The parameters of the µCT scan which will determine the minimum size of detected defects include resolution, signal to noise and bulk material properties[7].

For components exhibiting a considerable degree of porosity it is necessary to find a suitable algorithm to detect porosity from the µCT data and display the data for visualization. Suitable 3D image processing algorithms will be sensitive to the data filtering and thresholds selection. The porosity detection algorithm and the effect of changing parameters on number, volume and morphology of detected pores will be explored in this paper.

2 Additive manufacturing

Figure 1 shows the AlSi10Mg mirror specimen, which is manufactured using a commercially available selective laser melting (SLM) system. The mirror is approximately 40 mm in diameter and 6 mm thick consisting of a top layer, approximately 1 mm thick, linked via columns to a base layer approximately 1 mm thick. The mirror was scanned on a commercial µCT scanner resulting in 3D data for the entire sample with a pixel size of 30 µm. The top surface has been diamond turned to a mirror finish as described in Atkins *et al*[2].

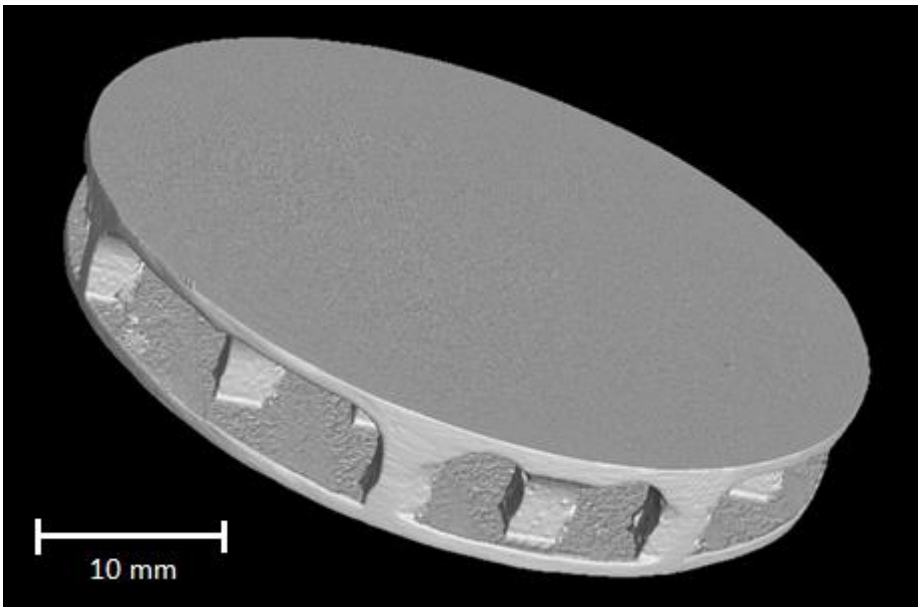

Figure 1 XCT image of diamond turned mirror

3 Pore analysis

The µCT data in Figure 2(a) shows the cross section of the top layer. It can be seen areas above the pillars show higher intensity in comparison to neighbouring regions. This variation in intensity is an artefact of the measurement rather than a real change in the material. As the method for locating porosity relies on intensity contrast this variation was removed using a 15 by 15 box filter to leave a uniform back ground as shown in Figure 2(b).

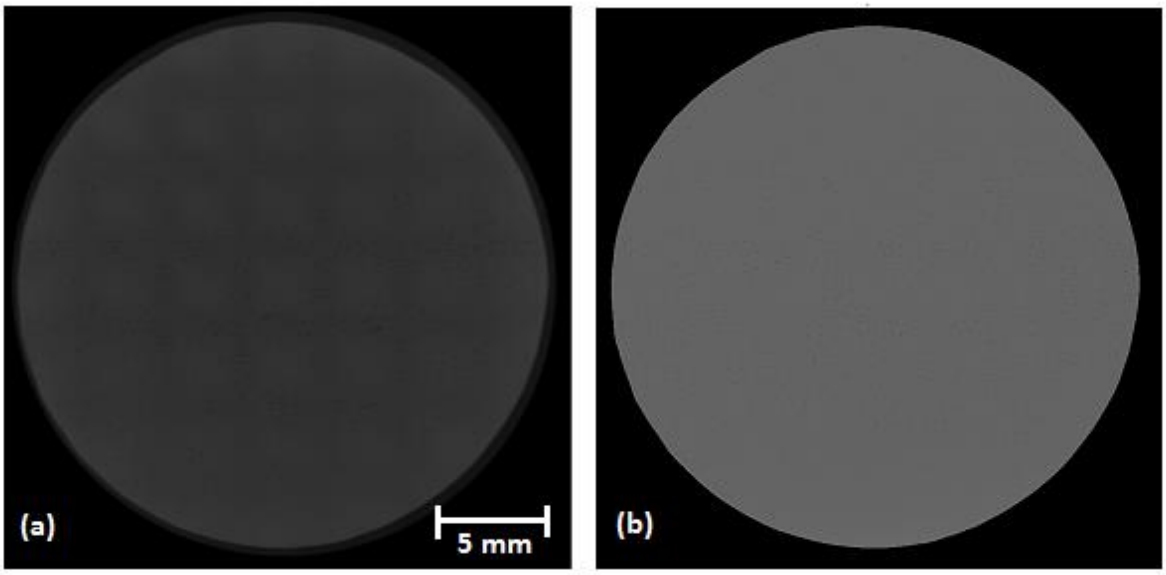

Figure 2 (a) Slice through top surface of planar mirror (b) Planar layer following application of box filter

The pores were extracted by applying an intensity threshold to the grey scale data in Matlab. This provided information about the locations of the porosity throughout the whole sample. Figure 3 shows the regions of porosity in red against the background of material in grey.

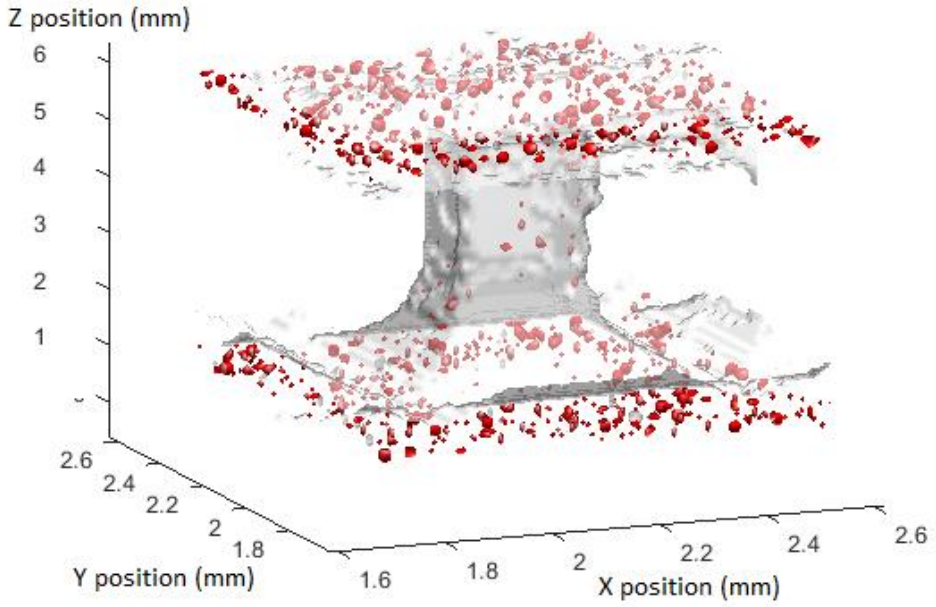

Figure 3 Volume around a single pillar with porosity shown in red

Figure 4 shows a 2D projection of the location of all pores within 1 mm layer of the top surface.

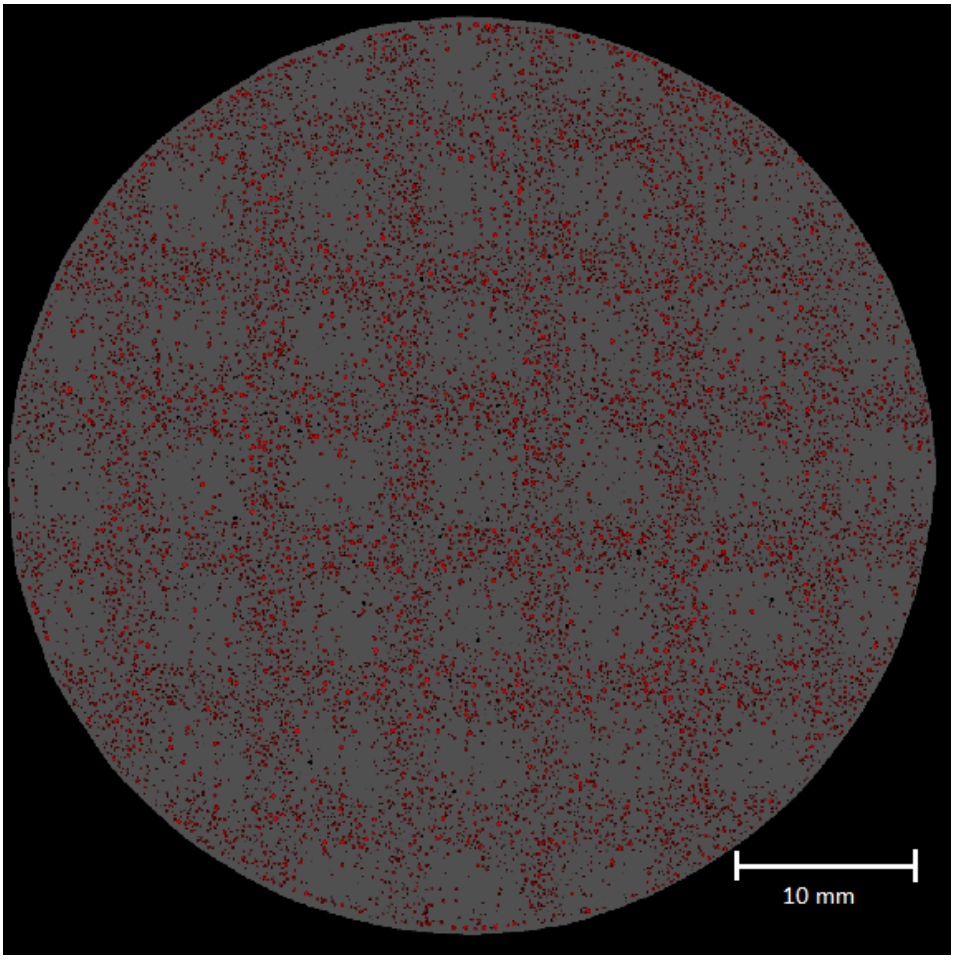

Figure 4 Porosity in top layer

It can be seen from Figure 4 that there is a lower level of porosity in the volumes above the support pillars. Figure 5(a) and (b) show a side views of the porosity with cross sections through the centre of the mirror structure.

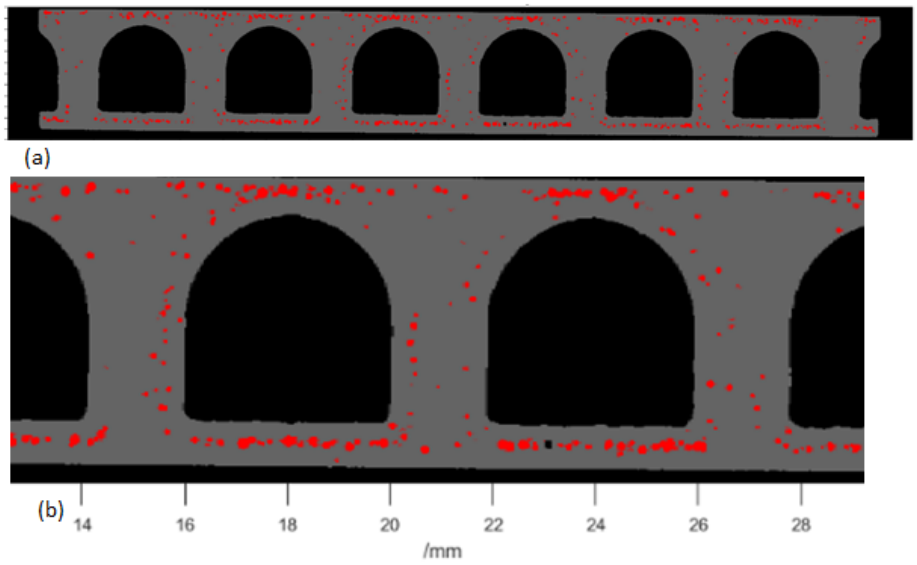

Figure 5 Porosity in cross section (a) Full view (b) Zoomed view

It is observed that the distribution of porosity in the top and bottom structures is not random but has the majority of the porosity lying in bands just below the top and bottom surfaces. A possible explanation for this lies with the hatching process used to consolidate the powder[8] as well as different regions experiencing variable thermal conductivity. As the back surface has not been diamond turned it provides an accurate guide to the depth below the surface at which the main pore layer forms.

Due to the limited system resolution and signal-to-noise ratio the probability that a pore of a given size will be detected (and the probability of a false detection per unit volume) will depend on the intensity threshold chosen. Figure 6 shows how the algorithm performs on the same area when used with varying intensity thresholds when the background intensity is adjusted to a grey scale level of 99. A high threshold of 93 will miss smaller pores but avoid false detections. A low threshold of 97 will detect smaller pores however will include false positive detections. A compromise value of 95 is also included. Further options for extending the robustness of this method include surveying the best threshold by performing higher resolution µCT scans on smaller samples of the mirror. The results of these measurements could be used to inform the most accurate choice for threshold. Improving the accuracy of the detection algorithm will improve the prediction of how the optical surface will perform.

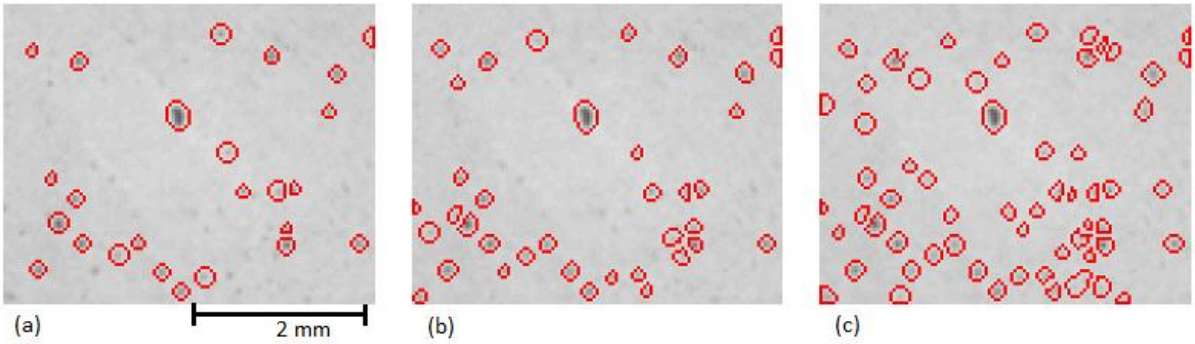

Figure 6 Pore detection for various thresholds (a) High threshold 93 (b) Medium threshold 95 (c) Low threshold 97

From the area analysed in Figure 6 the lower threshold detects 32 % fewer defects than the medium threshold and the higher threshold detects 41 % more defects. Further work will look to investigate standardized ways of calculating thresholds such as the Otsu method.

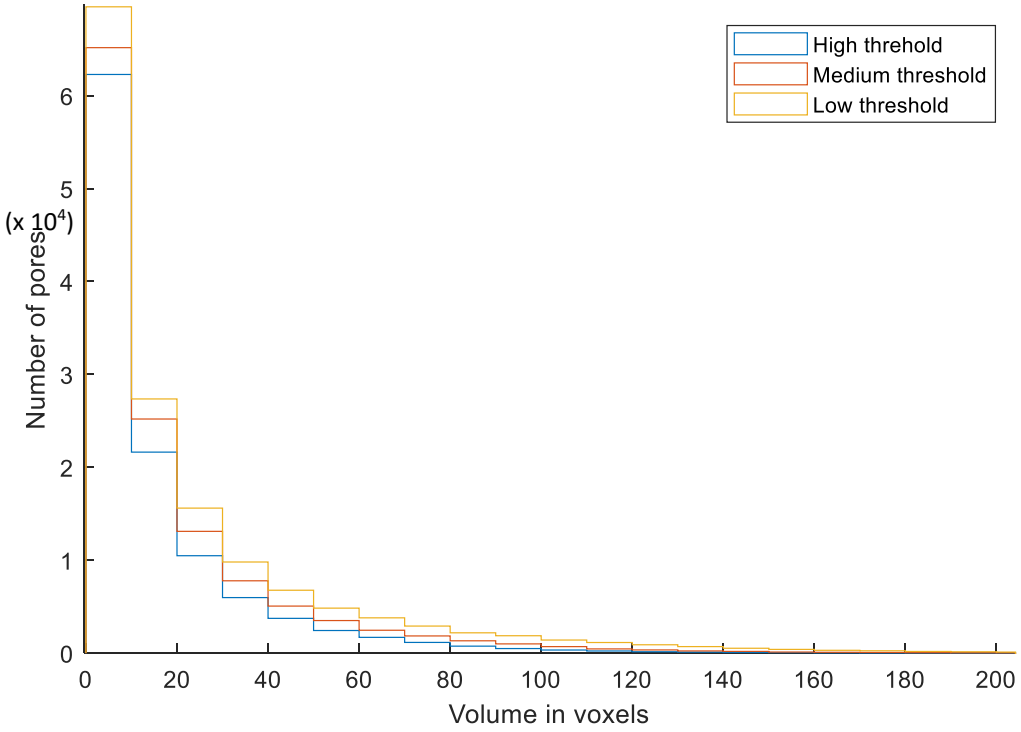

Figure 7 Volume histogram of pore

Figure 7 shows a histogram of all the detected pore volumes in the sample. The histogram demonstrates that the sample is dominated by pores of small/low volume. It is observed that the number of detected pores is dependent on the sensitivity of the detection algorithm. For pores close to the size of a voxel a more sensitive algorithm will result in more detected pores as smaller pores have a lower intensity contrast. The histogram shape for larger pores will be affected by intensity thresholding as their outer boundary will be smaller when the intensity threshold is set higher. This effect is shown in Figure 8 for a large pore.

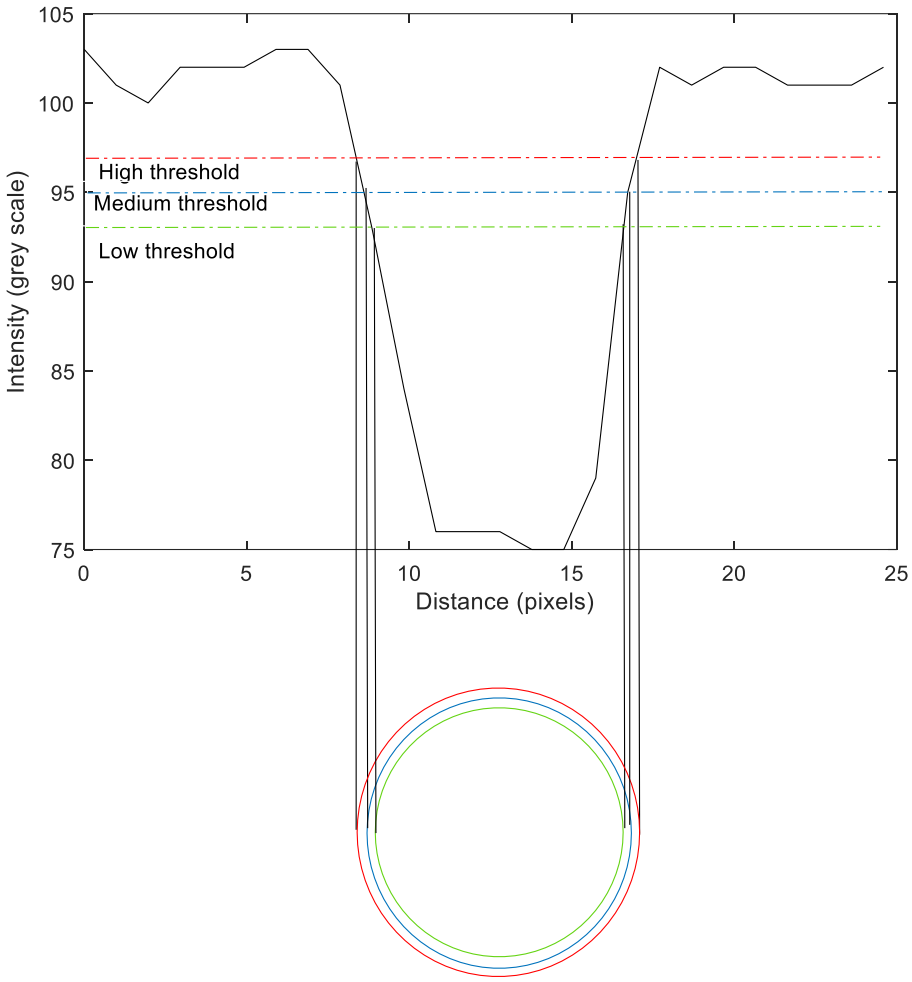

Figure 8 Effect of changing intensity threshold on detected pore size. With the high threshold the detected boundary is the red circle. With the medium threshold the boundary is the blue boundary. With the lower threshold the boundary is the green boundary.

There will also be a tendency for closely spaced pores to be merged when the threshold is set low resulting in detection of a larger volume pore.

4 Conclusion

An additive manufactured structure was analysed using µCT. Information on the distribution of porosity was obtained. This distribution indicates the pores preferentially form in layers approximately 0.5 mm deep beneath the surface. This information can provide feedback to AM manufacturers to understand how porosity affects the function of the finished build. The volume distribution of porosity was estimated and found to be dependent on the grey value thresholding of the algorithm. Further work in this area could include volume of porosities and its variation with respect to thresholding and cutting the sample to allow a higher resolution µCT scan. This high resolution scan could be used to guide selection of thresholding parameters for the whole sample scan.

5 References

1. Zhang, J. & Jung, Y.-G. Additive Manufacturing : Materials, Processes, Quantifications and Applications, Paperback ISBN: 9780128121559.

2. Atkins, C. et al. Topological design of lightweight additively manufactured mirrors for space. in Advances in Optical and Mechanical Technologies for Telescopes and Instrumentation III (eds. Geyl, R. & Navarro, R.) 15 (SPIE, 2018)

3. Kim, F. H. & Moylan, S. P. Literature review of metal additive manufacturing defects. Advanced Manufacturing Series (NIST AMS) - 100-16, (2018)

4. Tammas-Williams, S. et al. XCT analysis of the influence of melt strategies on defect population in Ti–6Al–4V components manufactured by Selective Electron Beam Melting. Mater. Charact. 102, 47–61 (2015).

5. Thompson, A., Maskery, I. & Leach, R. K. X-ray computed tomography for additive manufacturing: a review, Measurement Science and Technology, Volume 27, Number 7, 2016 .

6. Kasperovich, G., Haubrich, J., Gussone, J. & Requena, G. Correlation between porosity and processing parameters in TiAl6V4 produced by selective laser melting. Materials & Design, Volume 105, 5 September 2016, Pages 160-170 (2016).

7. Sun, W., Beown, S. & Leach, R. An overview of industrial X-ray computed tomography. NPL Report. ENG 32 (2012).

8. Martin, A. A. et al. Dynamics of pore formation during laser powder bed fusion additive manufacturing. Nat. Commun. 10, 1987 (2019).